Palaeogeography, Palaeoclimatology, Palaeoecology 585 (2022) 110716

Contents lists available at ScienceDirect

Palaeogeography, Palaeoclimatology, Palaeoecology

journal homepage: www.elsevier.com/locate/palaeo

Assessing the palaeohydrology of the lost Saraswati River in the Punjab-Haryana plains, Northwest India from satellite data

Zafar Beg, Kumar Gaurav *, Abhilash Singh, Sampat Kumar Tandon

Department of Earth and Environmental Sciences, Indian Institute of Science Education and Research Bhopal, Madhya Pradesh 462066, India

ARTICLE INFO

Editor: Dr. Paul Hesse

Keywords:
Palaeo discharge
Palaeo-channel
Rating curve
Dummy variable
Channel morphology

ABSTRACT

It has been suggested over a century ago that the Saraswati was a large river that flowed in the Sutlej-Yamuna interfluve, a region that is now devoid of any such large river system. This large river was commonly related to the Saraswati River described in the Rig-veda, and was correlated with the discovery of several Harappan sites in the region. Presently, there is only the ephemeral Ghaggar River that flows here with its limited discharge along the abandoned course of the 'lost' Saraswati. Also, it was hypothesised earlier that this region was drained by the waters from the drainage basins of both the glacier/monsoon-fed Sutlej and Yamuna rivers. It therefore stands to reason that this region should preserve evidence of the record of the past discharge variability that impacted this region prior to the major drainage reorganisation.

This study is an attempt to reconstruct the palaeohydrology of the Saraswati River. We investigate the hypothesis, that the ancient Saraswati River used to carry a combined flow of the Sutlej, Ghaggar and Yamuna river catchments. To examine this important question, we use the channel belt width, catchment area and average annual discharge of different rivers presently flowing on Indus-Ganga-Brahmaputra plains in the Himalayan Foreland. We use these variables to establish the empirical scaling relationships between the channel belt width and average annual discharge to the catchment area. We observed rivers having a larger catchment usually carry a higher discharge and have a wider channel belt. Finally, we use these empirical scaling relationships to estimate the channel belt width and average annual discharge of the lost Saraswati River at the time when it possibly carried the combined flow of the Sutlej, Ghaggar, and Yamuna rivers catchments. We obtained the average annual discharge of the Saraswati River of an order of 3000 $m^3 s^{-1}$ and channel belt width of about 11 km at the location downstream of the postulated confluence of the Sutlej and Yamuna rivers at Suratgarh.

1. Introduction

The lost Saraswati River has been postulated to be a large river system in the plains of North-West India. It has been posited in several studies (Kar, 2021; Singh et al., 2017; Clift et al., 2012; Danino, 2010; Valdiya, 2016; Radhakrishna and Merh, 1999) that this river flowed during the Late Pleistocene and Holocene, in the tract presently occupied by the Ghaggar-Hakra system (Fig. 1). Naruse (1985), Raikes (1968), Stein (1942) sought to connect the Harappan Civilisation to this large river. Initially, the hypothesis of a large river originating in the Higher Himalayas, and flowing through the Punjab-Haryana plain was advanced by R.D. Oldham of the Geological Survey of India in the latter half of the nineteenth century. More than a century later, this hypothesis of the lost Saraswati River that drained the Punjab-Haryana plain in the Sutlej-Yamuna interfluve continues to be explored by geoscientists, archaeologists, historians, and Indologists who are not only interested in the growth and demise of the Harappan civilisation, but in assessing the utility of palaeochannels in the management of groundwater resources in water-stressed regions (CGWB, 2016). These explorations have been intensified in the past few decades, particularly with the application of remote sensing technologies, subsurface geophysical methods for stratigraphic analysis, radiometric and luminescence chronology, and stable isotope analysis to this longstanding problem (Chatterjee et al., 2019; Clift et al., 2012; Giosan et al., 2012; Orengo and Petrie, 2017; Saini et al., 2009; Singh et al., 2017; Sinha et al., 2013; Kar, 2021). As a consequence of these investigations, that are spread over different areas of the Punjab-Haryana plain, the Thar in Rajasthan, and the Kutch region, a near-continuous about 1000 km palaeochannel from the Himalayan Mountain front downstream of Roopnagar in the Punjab-Haryana plains to Kutch (Fig. 1) has been reconstructed (Gupta et al., 2011, 2004;

* Corresponding author.
E-mail addresses: zafar17@iiserb.ac.in (Z. Beg), kgaurav@iiserb.ac.in (K. Gaurav), sabhilash@iiserb.ac.in (A. Singh), sktand@iiserb.ac.in (S.K. Tandon).

https://doi.org/10.1016/j.palaeo.2021.110716
Received 21 April 2021; Received in revised form 29 September 2021; Accepted 13 October 2021
Available online 27 October 2021
0031-0182/

Bhadra et al., 2009; Kar and Ghose, 1984; Rajawat et al., 2003, 1999). Most of the recent investigations (Clift et al., 2012; Giosan et al., 2012; Khonde et al., 2017; Singh et al., 2017) have however remained focused in either the Punjab-Haryana Plain or in Kutch, and the connectivity in the intervenient region of Rajasthan and the Thar is based on fragmentary evidence that needs further studies in order to establish the longitudinal connectivity of the postulated large Holocene/pre-Holocene river system (Saini et al., 2009; Chatterjee et al., 2019; Singh et al., 2017).

Some of the emphasis of the recent studies Giosan et al. (2012), Singh et al. (2017) has been on multidisciplinary investigations in the Punjab-Haryana Plain to understand the relationship of the various phases of growth and development of the Harappan Civilisation with a contemporaneous large river system in the region (Danino, 2010). Amongst other directions of research pursued by geoarcheologists in this region, they have, in particular, made attempts to understand the links between climate shifts in the Holocene with the different phases of the Harappan Civilisation-Early, Middle and Late, examining questions of habitability, human settlement patterns, and the resilience of human society to deteriorating climate condition, *i.e.* the weakening of the monsoon (Petrie et al., 2017; Giosan et al., 2012; Dixit et al., 2018).

Against the above background, an important question that is still being debated (Giosan et al., 2012; Singh et al., 2017) is the role played by basinal water resources and fluvial morphodynamics of the lost Saraswati River both in the growth and decline of the Civilisation. Earlier, Saini et al. (2009) through a detailed compilation and analysis of several dug wells, and borehole logs recognised relatively thick fluvial channel sand bodies in the sub-surface domain of the modern Ghaggar-Hakra basin of the Haryana plains and reconstructed buried channel networks at a sub-regional scale. This analysis, together with a luminescence chronology, based on a few dates, enabled them to infer that this region was occupied by a river system whose drainage area extended into the Higher Himalaya.

These predominantly (10–30) m thick grey salt and pepper micaceous sand bodies in the sub-surface were taken as evidence for the existence of a multi-channel drainage network of Higher Himalayan origin in these Plains. Further, based on the luminescence chronology, they argued that these buried palaeochannel systems pre-dated the Last Glacial Maxima. Additionally, Saini et al. (2009) also recognised a younger, much less developed fluvial regime in this region that was dated by them between 5.9 ± 0.3 ka and 2.9 ± 0.2 ka. This latter fluvial regime, according to Saini et al. (2009) included the palaeochannel segment mapped previously by (Yashpal, 1980), and considered to be a part of the lost Saraswati by them. Studies by Saini et al. (2009) have pointed towards a strong and pronounced shift in the palaeohydrological regime of the drainage network in the Haryana Plains dominated by Himalayan-fed fluvial system during the later part of marine isotope stage (MIS), and a much weaker subsequent fluvial regime in the mid- to late-Holocene. Subsequently, Sinha et al. (2013) based on electrical resistivity surveys together with the borehole subsurface stratigraphy, documented the presence of relatively thick fluvial sand bodies in the Ghaggar palaeovalley in the vicinity of some of the large Harappan settlements, such as Kalibangan. More recently, Chatterjee et al. (2019) based on luminescence dating reported the chronology of hydrological regime of the ancient river in the interfluve region. They suggested the recurrence of a large river due to the drainage reorganisation of the Sutlej River from 9 to 4.5 ka. According to these authors, this river flows during the Pre-Harappan phase and continued to support necessary water resources until the urban phase of the Harappan civilisation. They suggested this later fluvial regime corresponds to the Saraswati River.

Thus, in the past decade, several studies have suggested that the Sutlej and Yamuna rivers flowed in this interfluve region in the Late Pleistocene and Holocene along the present course of the modern Ghaggar River (Singh et al., 2017; Singh and Sinha, 2019; Chatterjee et al., 2019; Clift et al., 2012; Dave et al., 2019). The Sutlej River flowed into the main stem of the lost Saraswati River near Shatrana and the Yamuna River joined near Suratgarh (Fig. 1). Certainly, these rivers (Sutlej, Yamuna and Ghaggar) have been considered to contribute to the flow of the lost Saraswati River in the past. However, no detailed attempt has been made thus far to obtain an estimate of the discharge and relate it to the dimensions of this river.

Potter (1978) defined a large river based on the four attributes of (a) catchment area, (b) length of the river, (c) river discharge and, (d)

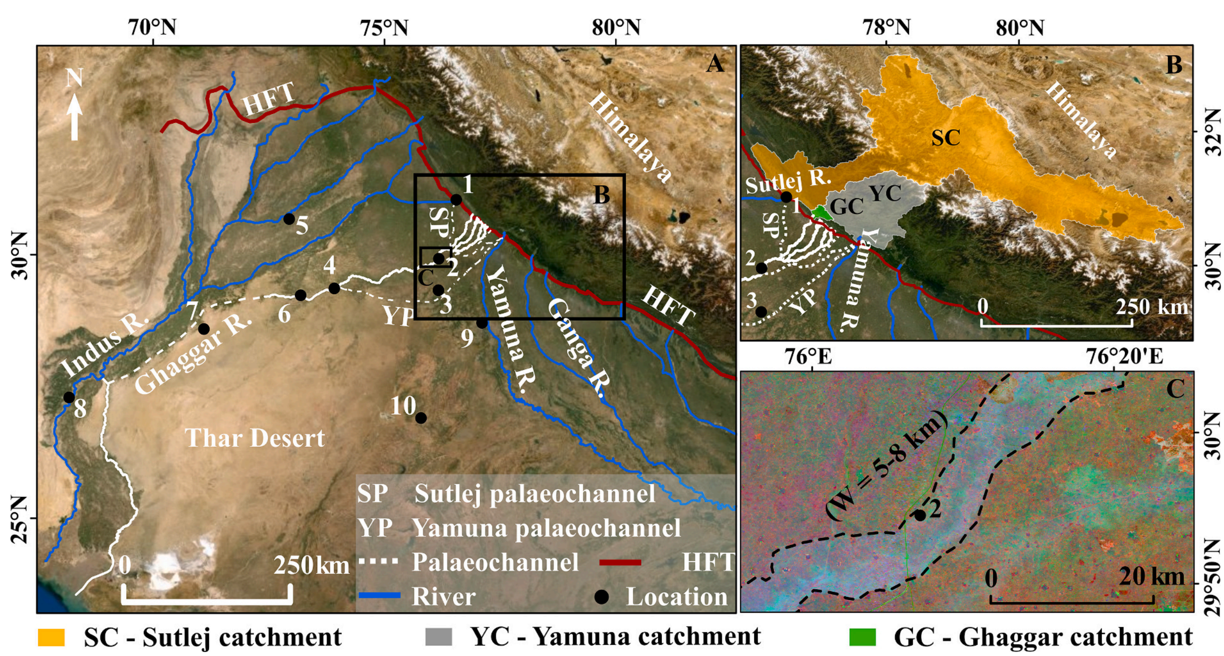

Fig. 1. (A) Palaeo-drainage map of the lost Saraswati River with the modern Himalayan rivers in North-West India. Black dots represent the locations - (1) Roopnagar, (2) Shatrana, (3) Rakhigarhi, (4) Suratgarh, (5) Harappa, (6) Anupgarh, (7) Ganweriwala, (8) Mohenjo-daro, (9) Delhi, (10) Jaipur. (B) Ancient fluvial system of the lost Saraswati River in the interfluve region (Yashpal, 1980). (C) Width of the Saraswati river palaeochannel (5-8 km) near Shatrana (image modified after; Orengo and Petrie, 2017).

annual sediment discharge. Large rivers can also be defined based on the size of channel dimensions (width and depth), sedimentary archives and preserved ancient delta deposits (Tandon and Sinha, 2007; Miall, 2006; Gupta, 2020). These parameters are often difficult to obtain for the inactive and abandoned rivers. This study attempts to obtain a first order estimate of the palaeohydrology of the lost Saraswati River. In doing so, we formulate two hypotheses; (1) the lost Saraswati River used to carry a combined flow from the contributing areas of the Sutlej, Ghaggar and Yamuna rivers in the Late Pleistocene, and (2) an estimate of this combined discharge can be obtained by comparing the hydraulic geometrical relationship of the modern rivers of the Himalayan Foreland with that of the postulated 'lost' Saraswati River.

2. Morphology of alluvial rivers

Alluvial rivers are self-formed, they adjust their geometry by erosion and accretion of the bed. The flow controls the fluvial incision which explicitly incorporates the role of changes in hydrological attributes of the channel such as the channel width, depth, velocity, and slope (Carling, 1988; Afshari et al., 2017; Dury, 1976). The bankfull discharge is an essential parameter that influences the channel adjustment in a river system (Faustini et al., 2009; Vianello and D'agostino, 2007). Generally, rivers with a larger catchment area produce larger discharges and eventually a wider channel belt (Bierman and Montgomery, 2014; Montgomery and Gran, 2001; Schumm, 1972). The adjustments in the river channels are complex and tend toward maintaining it in a state of equilibrium (Johnson and Fecko, 2008; Lecce, 2013).

Several studies have been conducted to understand the control of discharge on the channel geometry (Whitbread et al., 2015; Pavelsky et al., 2014; Doll et al., 2002). Leopold and Maddock (1953) established a set of empirical equations that characterised the spatial variation in channel behaviour of a natural river. These equations that define the functional relationship of hydraulic geometry of bankfull channel width (*W*), mean depth (*D*) and longitudinal slope (*S*) of a channel to the bankfull discharge (*Q*) are given below:

$$W = \alpha Q^{a} \tag{1}$$

$$D = \beta Q^{b} \tag{2}$$

$$S = \gamma Q^{c} \tag{3}$$

where α, β, γ and a, b, c are site specific constants and exponents. Subsequently, several workers have studied the feedbacks between catchment area, bankfull channel width and bankfull discharge in an inherently linked modern fluvial system (Faustini et al., 2009; Miller et al., 2013; Whipple, 2004; Whiting et al., 1999). Whipple (2004), Vianello and D'agostino (2007), Montgomery and Gran (2001) observed that the bankfull discharge and bankfull width of a river channel increases with the catchment area. Syvitski and Milliman (2007), Davidson and North (2009) reported that the variations in hydrological attributes (*Q* and *W*) depend in their response on the catchment area, and have strong correlations in many rivers belonging to different climatic and geological settings.

The coefficient and exponent of the rating curves established for the bankfull channel width (*W*) and bankfull discharge (*Q*) to the catchment area (*A*) of various rivers from different climatic and geological settings are reported in Table B.6 Appendix B.

Such empirical relationships serve as a valuable tool to obtain the first-order estimates of the unknown variable if the other parameters of the rating curve are known. Similar approach has been widely used to obtain the size (width, depth) and discharge of the ancient fluvial systems (Schumm, 1985).

Discharge estimates of inactive channels/palaeochannels can be reconstructed indirectly by inferring them from the size of the catchment area and width of a river. Several empirical studies have proven effective in studying the hydrology of the palaeochannels (Schumm, 1968; Davidson and North, 2009; Bhattacharya et al., 2016; Xu et al., 2017; Hesse et al., 2018). These studies rely on the surface relicts of the palaeochannel and their dimensions that are preserved in the alluvial plains (Hesse et al., 2018; Leigh and Feeney, 1995; Schumm, 1972). A few studies have used the rating curves established for the modern rivers to infer the hydrological attributes of the palaeochannels (Hayden et al., 2019; Hesse et al., 2018).

3. Study area

The Sutlej-Yamuna (S-Y) interfluve is located in the north-west part of the Indo-Gangetic Plain; it extends across Punjab, Haryana and Rajasthan and covers nearly 10^5 km^2 (Fig. 1). This region has low relief, with the elevation ranging from 150 to 350 m. The topographic orientation shows that the interfluve region has a predominant Northeast-Southwest gentle slope ($< 1^\circ$) with a mean direction of 216° (Roy et al., 2021).

This region receives about 70–80% rainfall during the Indian summer monsoon (Durcan et al., 2019; Kumar et al., 2014). The rainfall ranges from ~1200 mm/year near the Siwalik Hills to ~350 mm/year near the Thar Desert. The interfluve region encompasses diverse climatic setting, the northern part of the region comes under sub-tropical humid condition and the major part of the interfluve lies in semi-arid to arid region (Sinha et al., 2013; Saini and Mujtaba, 2012). Presently, two major glacial/monsoon-fed rivers, the Sutlej and Yamuna drain the margins of the S-Y interfluve. These rivers originate from the Himalayan hinterland and are connected to the Indus and Ganga river systems, respectively (Fig. 1). In the interfluve, a wide trace of a palaeochannel with a planform width ranging from (5 to 8 km) has been identified (Gupta et al., 2011, 2004; Singh et al., 2017). Several previous studies link this palaeochannel to the former course of the lost Saraswati River (Gupta et al., 2004; Chatterjee et al., 2019; Singh et al., 2017). As pointed out earlier, at present no major river flows in the S-Y interfluve, except the ephemeral Ghaggar River. This river originating from the foothills of the Lesser Himalaya has a catchment area of 480 km^2 at the Himalayan Front and an average channel width of about 100-200 m. This is a seasonal river and progressively loses its flow in the downstream. It drains from the confined valley of the sub-Himalayan region before emerging into the Himalayan foreland. Further, in the downstream, it is fed by the piedmonts and runs S-SW along a dominantly dry course of the channel/palaeochannel for about 300 km before being lost in the Thar Desert (Singh and Sinha, 2019; Saini et al., 2009). In addition, several defunct channels and palaeochannels that flow in the S-Y interfluve have been mapped using remote sensing data (Kar and Ghose, 1984; Mehdi et al., 2016; Orengo and Petrie, 2017; Kar, 2021). Recently, Roy et al. (2021) studied the orientation and trend of these palaeo channels based on stream orientation analyses; and showed that these are mainly oriented NE-SW indicating the predominant axis of the palaeochannel system.

4. Material and methods

4.1. Dataset

We have used Landsat images and Shuttle Radar Topography Mission (SRTM) Digital Elevation Model (DEM). These data were acquired from the United States Geological Survey (USGS) (https://earthexplorer.usgs.gov/). The Landsat mission provides consistent long-term images at spatial resolution ranges from (30 to 80) m with a temporal resolution of (16 – 18) days. We have downloaded 157 different images of the Landsat mission at an interval of 4–7 years from 1972 to 2019; this covers all the major rivers flowing in the Indus, Ganga, and Brahmaputra plains. These images correspond to post-monsoon period. We used these multi-temporal images to measure the channel belt width. Further, we have used the SRTM digital elevation model to delineate the catchment area of different rivers from a specific outlet point. Fig. 2 shows the detailed flowchart of the methodology. We acquired the average annual discharge of the Himalayan rivers from different sources. These correspond to discharge recorded at the gauge stations from the Central Water Commission (CWC), New Delhi, and Global River Discharge Database (GRDD). These agencies provide the discharge data at different temporal resolution, for example we could obtain ten days average discharge recorded at the gauge stations from CWC and average monthly discharge from GRDD. For some rivers, we have obtained the annual average discharge from the published literature. We have compiled the discharge data of 32 different rivers of the Himalayan foreland from the Brahmaputra plain in the east to the Indus plain in the west (Appendix B; Table B.7). We have then re-sampled the discharge data to obtain the annual average quantity.

4.2. Extraction of width and catchment area

We use Landsat satellite images and SRTM digital elevation model to extract the width of rivers and their catchment areas at the outlet. First, we identify the reach length of a river along which width is to be calculated. All the reaches that were selected on the rivers are located about 50 km downstream from the Himalayan Frontal Thrust (HFT). While selecting a reach on a river, we considered only those segments where no tributaries join or bifurcate and no structural interventions such as barrages or dams are present. We assumed that within the selected reach of a river, the discharge is conserved and there is no significant loss or gain of flow. Along the different rivers, the reach length varies from 10 to 40 km.

The width of a river observed from the top can be categorised into channel width, channel belt width, and valley width (Fig. 3 A). By definition, the channel width is a geomorphic feature in the fluvial plain which is controlled by the formative discharge (Wolman and Miller, 1960). The width of a channel belt corresponds to the boundary defined by the lateral migration of a river channel (Gibling, 2006). It is an integration of long-term fluvial activity in the region due to the corresponding long-term characteristics of the hydrological cycle. The valley

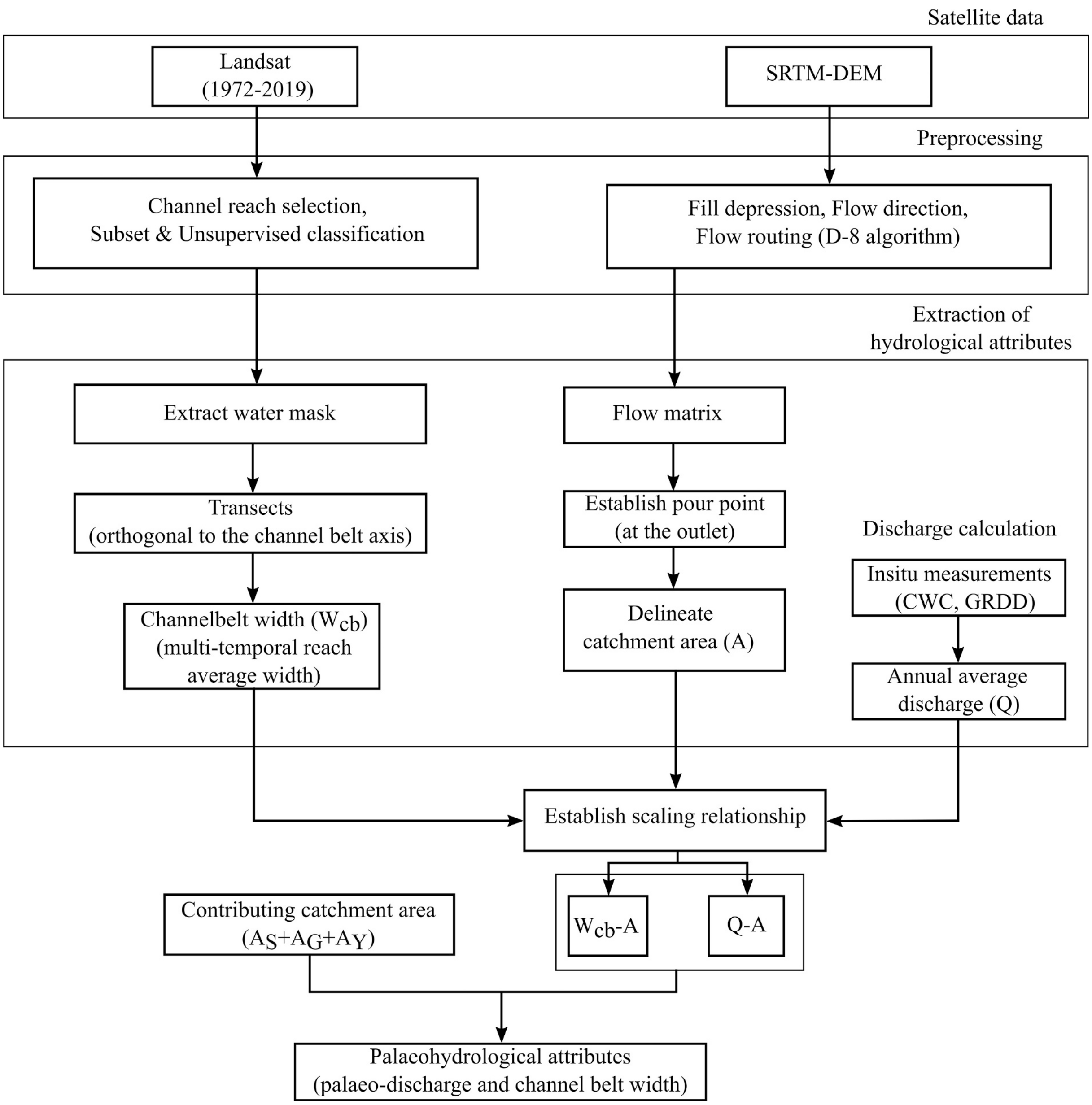

Fig. 2. Flowchart illustrates the processing steps of satellite images and the establishment of rating curves between channel belt width (W_{cb}) and average annual discharge (Q) to the catchment area (A). A_S, A_G, and A_Y correspond to the catchment area of the Sutlej, Ghaggar and Yamuna rivers respectively.

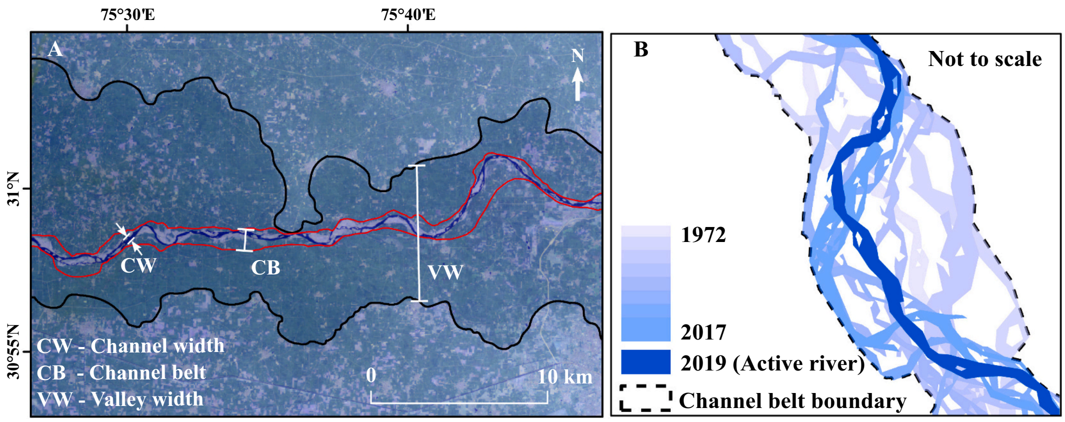

Fig. 3. (A) Conceptual diagram showing the channel width, channel belt width, and valley width identified with the help of satellite images and topographic (DEM) data, (B) Channel belt width is mapped by using the time series Landsat satellite images from 1972 to 2019. The channel belt boundary represents the extent of total lateral migration of channels during this period.

widths are the erosional land-forms formed by high magnitude events of long-term fluvial activity (Schumm and Lichty, 1965). The channel width and channel belt width can be extracted from the satellite images. Since the valley width is a flat corridor between the topographic elevated edges on both sides, it can be approximated using a DEM. In this study, we have considered the channel belt width for our purpose and extracted it using the Landsat satellite images.

4.2.1. *Channel belt width*

We use the Short-Wave Infrared (SWIR) band of Landsat images to measure the channel belt width of 26 different rivers from the Himalayan foreland (Appendix B; Table B.8). In SWIR, the water pixels appear dark which helps to distinguish the wet and dry pixels from the satellite images. On the raw SWIR images, we applied the unsupervised ISO-data algorithm to automatically create clusters with similar reflectance values. We then manually categorise these clusters into binary classes; water and non-water. The resulting binary images represent the water mask of the river. We use this mask to measure width along the selected reaches of the river channels.

Further, to measure the width of a channel belt, we use multi-temporal images of Landsat satellite mission. We extract the lateral extent of river migration by constructing a time series for 48 years (1972 – 2019) of the water mask for different rivers (Fig. 3 B). We consider the lateral extent of the river across the transects equivalent to the channel belt width. To measure channel belt width, we draw transects along the stream by keeping them orthogonal to the predominant axis of the channel belt. These transects divide each reach into at least ten individual measures, along which we calculate the average channel belt width of the river over a reach length.

4.2.2. *Catchment area*

We use SRTM digital elevation model to extract the catchment area of the rivers. We process the DEM to generate flow accumulation and direction grids. We then used the single flow (D-8) algorithm to generate a flow transfer matrix by converging the flow paths (Schäuble et al., 2008; O'Callaghan and Mark, 1984). We defined a pour point on the flow accumulation raster to extract the total contributing area at this location. The pour point serves as an outlet of the catchment where the surface water converges. Finally, corresponding to this outlet we extract the catchment area (Fig. 4).

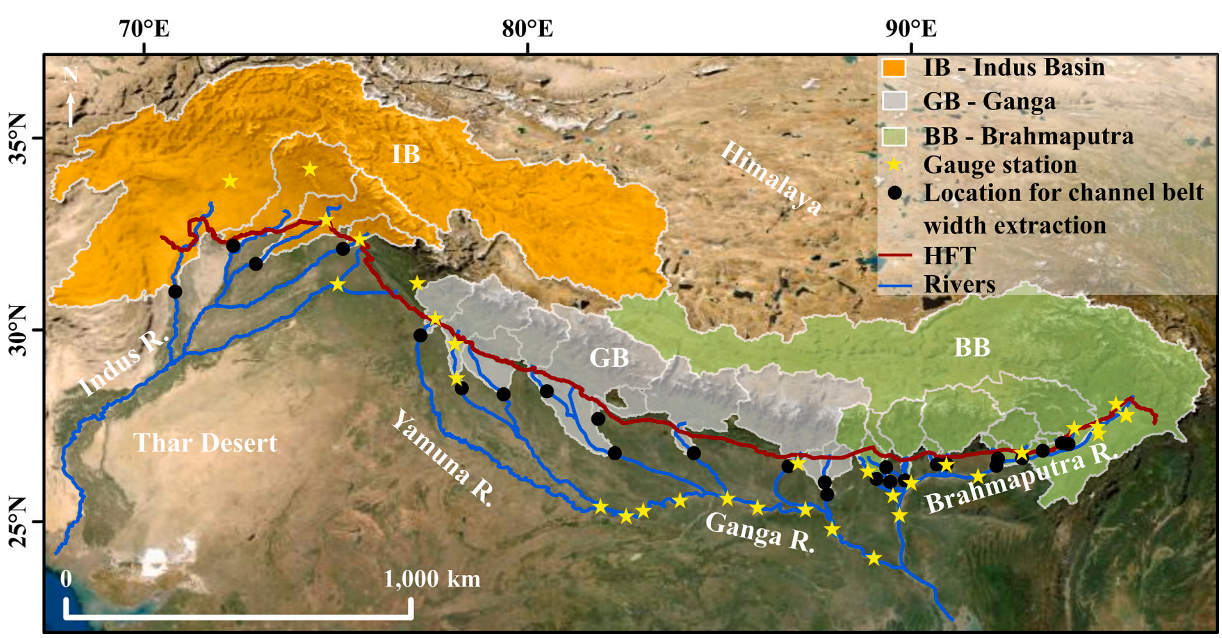

Fig. 4. The catchment of the Indus, Ganga, and Brahmaputra river basin. Circles in black (n=26) are the locations at which catchment area is extracted from DEM and channel-belt width is measured from satellite images. The stars in yellow represent the location of the gauge stations (n=32) at different rivers.

5. Establishment of scaling relationships

We use channel belt width, average annual discharge, and catchment area of the rivers to establish the empirical scaling relationships (Appendix B; Table B.7–Table B.8). To do so, we define the channel belt width (W_{cb}), catchment area (A) and average annual discharge (Q) in the dimensionless form. We do this by dividing the channel belt width (W_{cb}/d_{50}) and catchment area (A/d_{50}^2) by the median and square of the median grain size respectively. We defined the dimensionless water discharge as; $Q/\sqrt{gd_{50}^5}$ where d_{50} and $g = 9.8ms^{-2}$ are the median grain size and acceleration due to gravity respectively (Gaurav et al., 2017; Andrews, 1984; Ashmore and Parker, 1983).

We now plot the dimensionless channel belt width and average annual discharge of these rivers against the corresponding dimensionless catchment area on a log-log scale (Figs. 5 and 6). As expected, the rivers with a larger catchment area have a wider channel belt width and carry relatively higher discharge. Despite a considerable scatter, all the data points gather around a single power law curve. This observation suggests that despite the different geological and climatic settings of the Indus, Ganga, and Brahmaputra river basins, the empirical scaling relationship between the channel belt width vs. catchment area and average annual discharge vs. catchment area share a common regime equation.

6. Results and discussion

6.1. Distribution of hydrological attributes

The distribution of channel belt width, average annual discharge and catchment area of the rivers of the Indus, Ganga and Brahmaputra basins are summarised in the box plot (Fig. 7). These attributes show a large variation in their values (Appendix B; Table B.7–Table B.8). For example, the average width of the channel belt of the rivers ranges from 1 km to 14 km (Fig. 7 A). Most of these rivers (about 80%) have channel belt widths less than 5 km. Fig. 7 (B) highlights the large variability in the annual average discharge across the IGB basins. This ranges up to two orders of magnitude. The annual average discharge varies from 2×10^2 m^3s^{-1} (Jhelum River of the Indus basin) to 20×10^3 m^3s^{-1} (Brahmaputra River). We have observed that the annual average discharge of the Ganga and Brahmaputra basins shows a large variability as compared to the Indus basin. The catchment area of the sampled rivers varies about three orders of magnitude (Fig. 7 C).

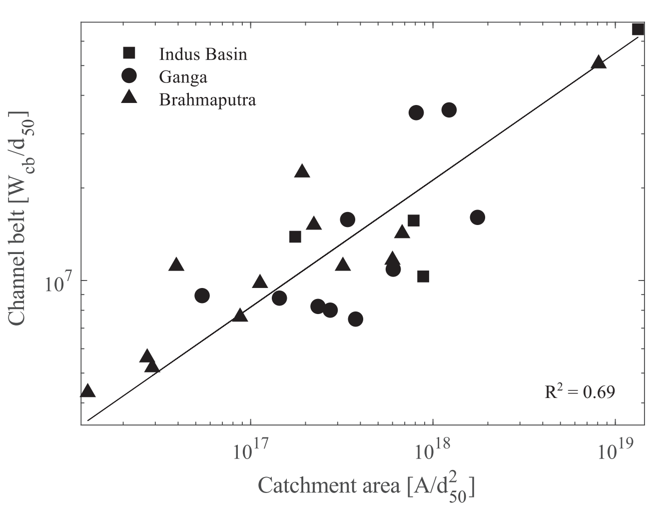

Fig. 5. Channel belt width-catchment area ($W_{cb} - A$) scaling relationships for the Himalayan Foreland Rivers. The solid black line shows RMA regression best fit.

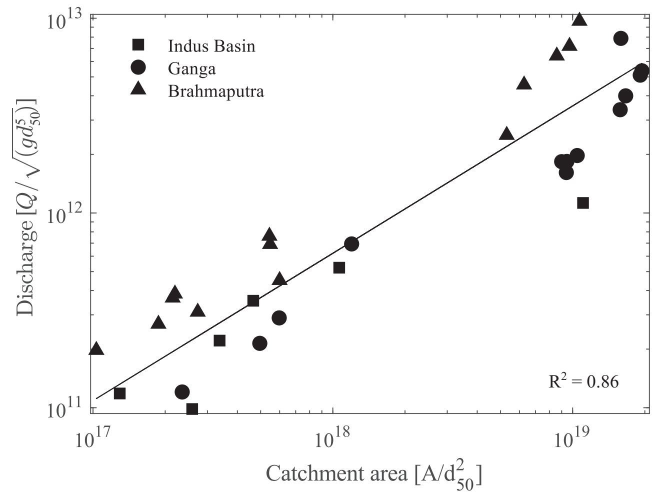

Fig. 6. Discharge-catchment area ($Q - A$) scaling relationships for the Himalayan Foreland Rivers. The solid black line is the best fit.

6.2. Scaling relationship

We plotted the average annual discharge and channel belt width of the rivers against their corresponding catchment area. We observed all the data points are clustered along a single line. This suggests that a common regime curve can be used to explain the functional relationship between average annual discharge-catchment area and channel belt width-catchment area of the rivers from the Indus, Ganga, and Brahmaputra basins.

To proceed further and test the emergence of a common regime relation, we now test the following null hypothesis: the regressions obtained for the channel belt width and average annual discharge of the Indus, Ganga, and Brahmaputra basins are not significantly different. Since we have a limited number of data points for the individual basins, they are insufficient for any statistical comparison. To overcome this problem, we performed the dummy variable regression analysis. This can be applied with few measurements as it facilitates to combine the categorical variable into a common regression (Garavaglia and Sharma, 1998; Splinter et al., 2010; Kolberg and Howard, 1995). This technique uses dummy variables as a set of categorical variables that allows us to integrate the qualitative (categorical or explanatory) variables in regression analysis (Gujarati et al., 2012; Cohen et al., 2013). The dummy variable is an independent variable that identifies the categorical membership and represents the values either 0 or 1 (Garavaglia and Sharma, 1998). A variable is coded “1” if it belongs to a given category; else it is “0”.

In the past, Wilkerson and Parker (2011), Rhoads (1991), have used dummy variable regression to test the difference in regression coefficients of best fit lines established for the sand bed and gravel bed streams. Kolberg and Howard (1995) used dummy variable to analyse the significance of sediment characteristics on Midwestern and Piedmont discharge-width relationship.

To apply dummy variable on our data, we use the Indus, Ganga, and Brahmaputra basins as categorical variables. Two dummy variables (D_1 and D_2) are used to denote I (Indus), G (Ganga) and B (Brahmaputra) basins for the regression analysis (Table 1). We considered the Brahmaputra basin as a control categorical variable because it has the maximum number of data points in its basin. For the control category, the dummy variable is coded as 0, and all other variables are compared with respect to the control variable (Gujarati et al., 2012; Cohen et al., 2013). Further, for Indus and Ganga basins, dummy variables are coded arbitrarily with the allowable value of either 0 or 1. Table 1 shows the coding schemes of the dummy variables (D_1 and D_2).

We now merge the data points of all the basins and obtain the best fit

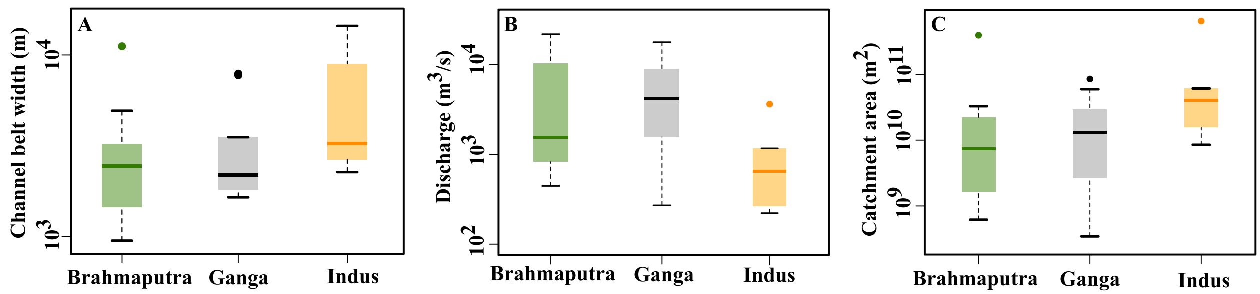

Fig. 7. Distribution of the channel belt width (A), average annual discharge (B), and catchment area (C) of the rivers from the Brahmaputra, Ganga, and Indus basins. Horizontal line in the box plots is the median value, shaded portions is the interquartile range, dotted line is the whiskers that is extended to a maximum and minimum values of the data set, and the circles show the outliers.

Table 1
Coding schemes for the dummy (D_1 *and* D_2) variables. The shaded region represents the control category.

Category	Dummy variable (D_1)	Dummy variable (D_2)
Indus basin (I)	1	0
Ganga basin (G)	0	1
Brahmaputra basin (B)	0	0

line between the dependent variables (channel belt width and average annual discharge) and independent variable (catchment area). The general form of the regression equation obtained from the dummy variable regression model reads;

$$log_{10}y = \beta_0 + \beta_1 log_{10}x + \beta_2 D_1 + \beta_3 D_2 + \beta_4 D_1 log_{10}x + \beta_5 D_2 log_{10}x \quad (4)$$

where x and y are the independent and dependent variables respectively, D_1 and D_2 are dummy variables for the categorical variable and β_0 to β_5 are the regression coefficients. A detailed procedure of dummy variable regression is provided in Appendix A. Table 2 gives the regression coefficients for W_{cb}-A and Q-A obtained from the dummy variable regression.

Finally, we performed the Analysis of Variance (ANOVA) to test the similarity of regression coefficients (intercept and exponent) of the Indus, Ganga and Brahmaputra basins obtained from dummy variables regression. We observed that the dummy variable regression coefficients of the Indus, Ganga, and Brahmaputra basins cannot be differentiated within the 95% level of confidence (Table 2).

This suggests we can consider our data points as a representation of the same population. We now plot the channel belt width and average annual discharge of the basins together as a function of their corresponding catchment area on log-log scale (Figs. 5 and 6).

To obtain the best-fit line, we perform the Reduced Major Axis regression (RMA) on the logarithm of channel belt width and average annual discharge (Sokal and Rohlf, 1995; Gaurav et al., 2015, 2017). The correlation of channel belt width and average annual discharge against the catchment area is significant at the 95% level of confidence. Table 3 gives the intercept (α) and exponent (β) of the regime curves. The quality of regression (R^2) is 0.86 for the average annual discharge-catchment area and 0.69 for the channel belt width-catchment area.

The coefficients and exponents of our regime curves for the channel-belt width and average annual discharge to the catchment area are in accordance with the values obtained for the river basins of different climatic and geologic settings worldwide (Frasson et al., 2019; Vianello and D'agostino, 2007; Faustini et al., 2009). For example, globally it is observed that the exponent of the discharge-catchment area curve varies in the range between 0.72 to 1 (Appendix B; Table B.6). In our case, we obtained the exponent value "β_Q = 0.77" for the average annual discharge-catchment area curve. This lower value indicates that the discharge in the Himalayan Foreland Rivers is produced at a relatively lower rate per unit catchment area.

Table 2
Summary of the dummy variable multiple linear regression (MLR) and ANOVA for $W_{cb} - A$ and Q - A scaling relationships.

Coefficients	$W_{cb} - A$	$Q - A$	p-value	
			$W_{cb} - A$	$Q - A$
β_0	1.23	-2.31	0.32	0.02
β_1	0.34	0.80	0.00	0.00
β_2	-1.09	2.54	0.69	0.17
β_3	-0.82	-0.58	0.76	0.67
β_4	0.06	-0.16	0.70	0.12
β_5	0.04	0.01	0.78	0.90

6.3. Palaeo-discharge of the Saraswati River

We now use the regime curves established for the modern rivers of the Himalayan Foreland basins to obtain an estimate of the average annual discharge and channel belt width of the lost Saraswati River. In doing so, we extract the catchment area of the Sutlej, Ghaggar, and Yamuna rivers from the digital elevation model obtained from the Shuttle Radar Topographic Mission (SRTM).

The contributing area of a river channel increases from upstream to the downstream. It is therefore important to locate the pour point at the

Table 3
The coefficients of regression analysis with 95% confidence interval.

Method	Relationship	No. of sample	Intercept (α)	Exponent (β)	R^2
RMA	$W_{cb} - A$	26	-0.04	0.41	0.69
	$Q - A$	32	-2.01	0.77	0.86

location on the river above which the catchment area is to be calculated. Keeping this in mind, we have selected the pour points near Shatrana (postulated confluence with the Sutlej River) and Suratgarh (postulated confluence with the Yamuna River) to calculate the catchment area of the Ghaggar river (Clift et al., 2012; Singh et al., 2017). This allows us to know the catchment area of the Ghaggar River above Shatrana and Suratgarh in the interfluve region.

Recently, Roy et al. (2021) have reported that in the interfluve, the existing drainage's have deviated from the orientation of the palaeo-channels and the regional slope. This drainage reorganisation is perhaps due to the climatic and geological events (Van Der Beek et al., 2002). We could not extract the flow matrix at the postulated confluences of the Sutlej and Yamuna River with the lost Saraswati River. This limits us to extract the catchment area of the palaeo-Sutlej and palaeo-Yamuna at their confluences with the Ghaggar River near Shatrana and Suratgarh respectively.

Therefore, to obtain an approximation of the catchment area for both Sutlej and Yamuna rivers, we transfer the pour point at an equivalent point on the present-day existing flow matrix (Fig. 8). We establish the pour points on both the rivers at the location where drainage orientation changes along its present course (*i.e.* avulsion nodes).

Finally, using the catchment area of individual basins, we estimate their channel belt width and average annual discharge using the regime equations. Further, following the hypothesis that once the Saraswati River used to carry the combined flow of the Sutlej, Ghaggar, and Yamuna rivers catchment (Clift et al., 2012; Yashpal, 1980; Saini et al., 2020; Kar, 2021), we sum the estimated discharge of these rivers to obtain a possible combined discharge of the Saraswati River. This provides a discharge estimate of the lost Saraswati River of the order of 3000 m^3s^{-1} at Suratgarh. Similarly, using our regime curve we obtained the channel belt width of the Sutlej, Ghaggar, and Yamuna rivers at the outlet of their corresponding catchment area. We then sum the individual widths to obtain the channel belt width downstream of the confluence. We obtained the channel belt width of the lost Saraswati river close to 11 km after the confluence of the Ghaggar and palaeo-Yamuna Rivers near Suratgarh.

Though these estimates carry large uncertainties, they still provide a first-order estimate of the palaeo-hydrology of the lost Saraswati River. At present, the Sutlej and Yamuna rivers are the major tributaries of the Indus and Ganga rivers respectively. The present-day average annual discharge of the Sutlej and Yamuna rivers at Roopnagar and Hathnikund barrages is about 500 m^3s^{-1} and 270 m^3s^{-1} respectively. We observed that the combined average annual discharge of these rivers is substantially lower (one fourth) as compared to the discharge of the palaeochannels estimated using our rating curve.

We believe that the intensified precipitation derived from Indian Summer Monsoon (Dixit et al., 2018) and flow from Himalayan Glacier (Singh et al., 2016) in the past could be a reason for this large difference in the hydrology of the palaeochannels in the Sutlej-Yamuna interfluve and the modern rivers in the Himalayan Foreland. Further, in-spite of significant differences, the hydrology of the lost Saraswati River can be compared to the present day large rivers of the Himalayan Foreland (Appendix B; Table B.7 and Table B.8).

Earlier Maemoku et al. (2012) compared the floodplain and the annual average discharge of the Indus River and its major tributaries in the Punjab plain. They observed the average floodplain width of the Ghaggar River is about 5 km, which is significantly smaller than the average floodplain width (10–20 km) of the major rivers of the Indus basin. Based of this evidence, they concluded that the Ghaggar floodplain is too small to explain the discharge of the large rivers of the Himalayan origin.

Recently, Singh et al. (2017) have reported the presence of a large channel belt width. Previous workers have measured this width using different approaches; such as, remote sensing (Gupta et al., 2011; Mehdi et al., 2016), sedimentary well logs (Singh et al., 2017) and electrical resistivity method (Sinha et al., 2013). We found that the channel belt width of the Saraswati palaeochannel that we have estimated using our approach broadly compares with the width of the Saraswati River reported by the previous workers (Table 4).

6.4. Fluvial morphodynamics of the Saraswati River

Previous studies have reported the evolution of drainage in the Sutlej-Yamuna interfluve. Based on provenance studies that relied on U-Pb zircon dating, Clift et al. (2012) suggested that the Sutlej and Yamuna rivers had flowed on the interfluve region during the pre-LGM period. They reported Yamuna River flowed along the course of Chautang River and joined the Ghaggar River near Suratgarh. Further, they suggested

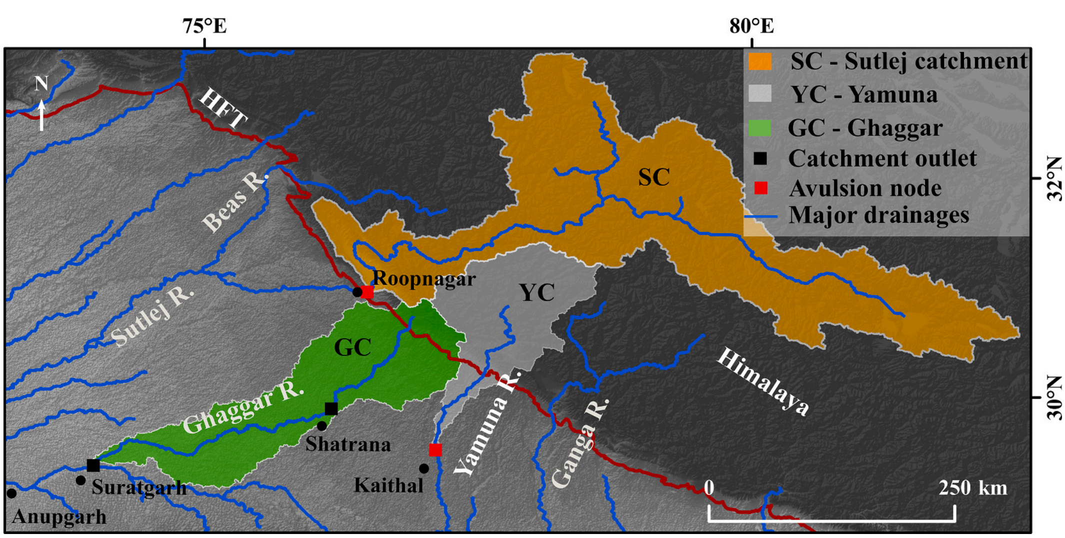

Fig. 8. Present-day drainage's on the S-Y interfluve. Avulsion nodes(in red square) of Sutlej and Yamuna rivers (proposed by Clift et al. (2012) and Singh et al. (2017)). We have considered these outlet points to approximate the catchment area of the palaeo-Sutlej and palaeo-Yamuna rivers at the confluence near Shatrana and Suratgarh respectively.

Table 4
Estimated width of the Saraswati River palaeochannels reported by the previous workers using different techniques.

Approach	Data used	Width (km)	Remarks	Location	Source
Remote Sensing	IRS P3 WiFS	4-10	Channel width	Sirsa via Anupgarh to Rann of Kutch	Gupta et al. (2004)
	Landsat ETM+	8	Valley width	Sirsa to Hanumangarh	Mehdi et al. (2016)
	Landsat TM	5-6	Channel belt	Himalayan front (Roopnagar) to Thar Desert	Singh et al. (2017)
Well logs	Subsurface sand bodies	> 8	Channel belt	Kalibangan	Singh and Sinha (2019)
	Subsurface sand bodies	> 5	Channel belt	Kalibangan	Singh et al. (2017)
	Subsurface sand bodies	5-10	Aquifer extent	Shatrana and Fatehabad	Van Dijk et al. (2016)
Electrical Resistivity and Well logs	Subsurface sand bodies	> 12	Channel belt	Moonak and Kalibangan	Sinha et al. (2013)
	Subsurface sand bodies	14	Aquifer extent	Cholistan (Downstream of suratgarh)	Geyh and Ploethner (1995)
Rating curves/Remote sensing	In-situ discharge, SRTM-DEM, and Landsat (MSS - OLI and TIRS)	7 11	Channel belt Channel belt	Shatrana Suratgarh	This study

avulsion of the Yamuna River from the Saraswati River to its present course is episodic in nature and occurred approximately during 49 ka to 10 ka. Recently, Dave et al. (2019) based on optically stimulated luminescence (OSL) dating suggested that the Yamuna River (Chautang) ceased its flow to the Saraswati River most likely around 40 – 45 ka. On the other hand, the Sutlej River contributed to Ghaggar River near Shatrana and flowed until 10 ka (Singh et al., 2017). The Sutlej River has shifted from the Saraswati River to its present course prior to 8 -10 ka (Singh et al., 2017). Further, it was suggested that the shifting of the course of the Sutlej River is possibly related to multi-staged avulsions that extended over millennial timescales (Roy et al., 2021). Also, earlier it has been suggested that only a rain-fed river flowed in the interfluve region during the Holocene and later this river become ephemeral as monsoon weakened in this region (Giosan et al., 2012).

Based on the studies discussed above, three possible main scenarios can be envisioned for the hydrological regime and the drainage reorganisation of the interfluve that hosted the Saraswati River; (a) the Sutlej, Yamuna, and Ghaggar rivers flowed together in the interfluve region along the course of the lost Saraswati River, (b) the Sutlej and Ghaggar rivers drain through the Saraswati River palaeochannel, and (c)

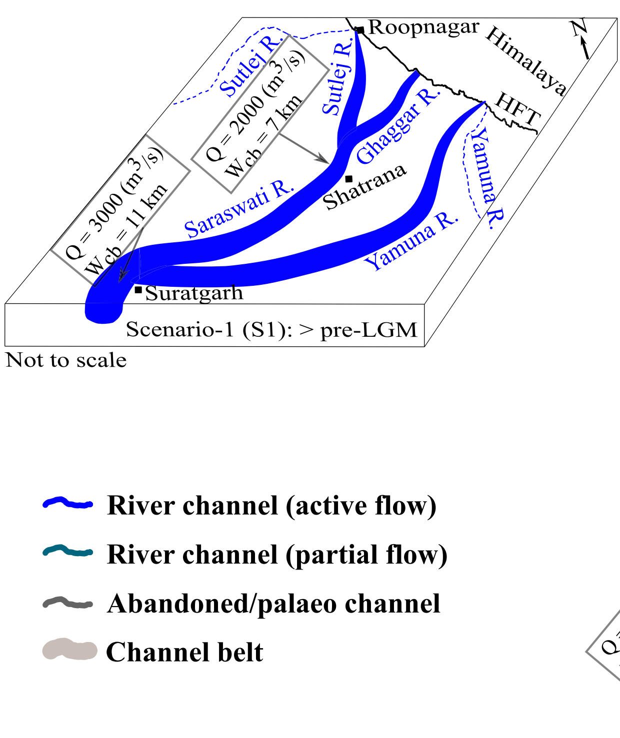

Fig. 9. Conceptual diagram to illustrate the drainage dynamics of the Saraswati River in different geological time period in the Sutlej-Yamuna interfluve. Drainage evolution is conceptualised through different scenarios (S1-S3). Scenario-1 (S1) shows the existence of a large fluvial system during the pre-LGM period. It is believed that during this period the Sutlej, Yamuna, and Ghaggar rivers used to drain through the Saraswati palaeochannel (Clift et al., 2012). Scenario-2 (S2) represents the avulsion phase (during 20 ka to 8 ka) of the Yamuna River (Clift et al., 2012; Dave et al., 2019). In this period Sutlej and Ghaggar rivers used to drain through the Saraswati palaeochannel (Singh et al., 2017). Finally the scenario-3 (S3) shows the limited flow after the complete avulsion of glacial-fed Sutlej and Yamuna River in the Holocene (<4 ka) (Singh et al., 2017; Giosan et al., 2012).

Table 5
Estimates of the discharge and channel belt width of the Saraswati River at the postulated confluences of the palaeo-Sutlej and Ghaggar rivers near Shatrana and the palaeo-Yamuna to the main stem of the lost Saraswati river near Suratgarh. The estimates of channel belt width and average annual discharge is obtained for the three possible scenarios (Fig. 9) postulated by the earlier researchers.

Scenario	Hypothesis	Period	Contributing river	Attributes			Description
				Measured	Estimated		
				A(km^2)	W_{cb}(km)	Q (m^3s^{-1})	
	The confluence of Sutlej and Ghaggar River near Shatrana (Singh et al., 2017)		Sutlej	58×10^3	5.0	1500	Estimates at the downstream of Shatrana; a postulated confluence of the palaeo-Sutlej and Ghaggar rivers near Shatrana (Fig. 9; S1)
			Ghaggar	5×10^3	2.0	300	
			Total at Shatrana (approx.)	63×10^3	7.0	2000	
S1	The confluence of Yamuna River to the Saraswati in the downstream of Shatrana near Suratgarh (Clift et al., 2012)	pre-LGM	Yamuna	13.5×10^3	2.5	500	Estimates at the downstream of Suratgarh; a postulated confluence of the palaeo-Yamuna with the main stem of the lost Saraswati River in the downstream of Shatrana (Fig. 9; S1)
			Sutlej	58×10^3	5.0	1500	
			Ghaggar	22.5×10^3	3.5	1000	
			Total at Suratgarh (approx.)	94×10^3	11	3000	
			Sutlej	58×10^3	5.0	1500	
S2	A scenario when the lost Saraswati River used to receive a much reduce flow from the Yamuna river near Suratgarh. During this period the main flow was through the Sutlej and Ghaggar rivers (Clift et al., 2012; Dave et al., 2019; Singh et al., 2017)	between 20 ka to 8 ka	Ghaggar	22.5×10^3	3.5	1000	Estimates at the downstream of Suratgarh (Fig. 9; S2)
			Total at Suratgarh (approx.)	80×10^3	8.5	2500	
S3	A period when the palaeo-Sutjej river completely avulsed and only the Ghaggar River was contributing to the flow of the lost Saraswati River (Singh et al., 2017; Giosan et al., 2012)	< 4 ka	**Ghaggar at Suratgarh (approax.)**	22.5×10^3	3.5	1000	Estimates at the downstream of Suratgarh (Fig. 9; S3)

only the Ghaggar River used to contribute to the Saraswati River (Fig. 9 and Table 5). Further, based on these scenarios, we evaluate the three different outcomes for the palaeohydrology of the lost Saraswati River.

Considering our first hypothesis, *i.e.* the 'lost' Saraswati River used to carry the combined flow of the catchments of the Sutlej, Yamuna, and the Ghaggar rivers, we estimated the channel belt width and average annual discharge of the Saraswati River using our rating curves at Suratgarh and Shatrana. This phase is represented by the scenario-1 (S1) which shows the existence of a large fluvial system in the interfluve region (Fig. 9 S1). Assuming this scenario, we obtained the channel belt width of about 11 km and discharge 3000 m^3s^{-1} in the downstream of Suratgarh. In the reach between the confluence of Sutlej and Ghaggar rivers at Shatrana and before the confluence of Yamuna and Ghaggar rivers at Suratgarh, we obtained the channel belt width of about 7 km and average annual discharge 2000 m^3s^{-1} (Table 5). Our estimates of channel belt width accords well with the previous findings using different remote sensing and stratigraphic approaches (Table 4) (Sinha et al., 2013; Singh et al., 2017; Mehdi et al., 2016; Gupta et al., 2011; Singh and Sinha, 2019). Further, comparison with the modern perennial rivers of the interfluve (Sutlej and Yamuna) shows that our discharge estimates of the lost Saraswati River are higher by a factor of four. In addition about 50% of the present day rivers on the Himalayan Foreland have a lesser average annual discharge as compared to the estimate for the lost Saraswati River (Table B.7 in Appendix B). Bookhagen et al. (2005) and Scherler et al. (2015) have suggested that the higher discharge and sediment flux in the interfluve rivers (Sutlej and Yamuna) was due to the enhanced precipitation in the Late Pleistocene (29 – 24 ka) and Holocene (10 – 4 ka).

Now we consider the second hypothesis which suggests that after the avulsion of the Yamuna River, only the Sutlej and Ghaggar rivers used to contribute to the flow of the Saraswati River. This scenario (S2) has remained similar in the Shatrana-Suratgarh reach, we observe notable change downstream of Suratgarh owing to the losses related to the contributions from the palaeo-Yamuna river. We found a reduction in average annual discharge 2500 m^3s^{-1} downstream of the palaeochannel confluence at Suratgarh (Table 5 & Fig. 9 S2).

Finally as per scenario (S3), we estimate the average annual discharge of the Saraswati River assuming the flow only from the Ghaggar River after the avulsion of Sutlej River (Fig. 9 S3). This results into a significant reduction in average annual discharge (about 300 m^3s^{-1}) and channel belt width (2 km) of the Saraswati River (Table 5). Estimated discharge is lower than the average annual discharge of any glacial-fed river presently found on the Himalayan Foreland. Later, during the arid phase of the Holocene (Meghalayan Stage), a weakened monsoon together with reduction in discharge because of avulsion of the Sutlej river resulted in the transformation of the Saraswati River from a large Himalayan-fed river prior to mid-Holocene to an ephemeral river (Chatterjee et al., 2019; Giosan et al., 2012; Singh and Sinha, 2019; Singh et al., 2017). These major regional environmental changes then caused the decline of the Harappan Civilisation in the region.

Recently, Singh et al. (2021) have reconstructed the palaeohydrology of the foothills Markanda River. They reported the palaeo-discharge of the Markanda River to be about 4600 m^3s^{-1} during the Late Holocene (S3 in this study). This is about 15–18 times higher than the peak summer as well as the 100 year return period discharge of the present-day Markanda River.

According to our approach, we obtained an average annual discharge of about 300 m^3s^{-1} near Shatrana and about 1000 m^3s^{-1} near Suratgarh. Interestingly, the value of 300 m^3s^{-1} downstream of Shatrana compares in order of magnitude with the 100 years return period discharge and the peak discharge during the summer monsoon as reported by Singh et al. (2021). However, we found a large difference in the palaeo-discharge estimated in this study and the one estimated by Singh et al. (2021). This large difference is possibly due to different approaches used to estimate the palaeo-discharge. It is important to note that the discharge that Singh et al. (2021) have reported corresponds to the palaeo-flood value; whereas our estimates of the discharge corresponds to the formative discharge that has set the channel belt.

7. Conclusions

With the ultimate objective of obtaining estimates of the palaeohydrology of the lost Saraswati river, this study derives a set of empirical relationships from the parameters (W_{cb}, Q, and A) using the modern river systems of the Indus, Ganga, and Brahmaputra basins. The results showed that the channel belt width and average annual discharge are positively related with the catchment area and provide strong correlation with coefficient of determination of 0.86 and 0.69 for the average annual discharge-catchment area and channel belt width-catchment area respectively. This suggests the regression equations developed for $W_{cb} - A$ and $Q - A$ relationships provide first-order estimates of channel belt width and average annual discharge.

This study also investigated the apparent difference in the regression coefficients among the basins using the dummy variable regression. Our analysis demonstrates that the regression coefficients are invariable among the basins. This finding remains consistent across 2 orders magnitude of the average annual discharge and 3 orders of magnitude in the catchment area. This allowed us to suggest that the $W_{cb} - A$ and $Q - A$ relationships developed here follow a similar scaling law across the basins.

Finally, we have estimated the palaeo-discharge of the Saraswati river from the average annual discharge-catchment area relationship developed in this study. The palaeo-discharge magnitude of pre-Early Holocene scenarios is 3–4 times that of present-day interfluve rivers (Sutlej and Yamuna) strongly suggesting major drainage reorganisation in this interfluve region in the mid- to late Holocene. The estimated channel belt width obtained in this study shows broad convergence with the estimates obtained from previous stratigraphy-based studies that have shown channel belt width up to 8–10 km in this interfluve region.

Declaration of Competing Interest

The authors have no conflicts of interest to disclose.

Acknowledgements

We acknowledge IISER Bhopal for providing institutional support. Zafar Beg's PhD is supported through the Institutional fellowship of IISER Bhopal.

Appendix A. Statistical analysis

We have used the log transformed hydrological variables. Therefore for $W_{cb} - A$ the Eq. (4) takes the following form

$$log_{10}W_{cb} = \beta_o + \beta_1 log_{10}A + \beta_2 D_1 + \beta_3 D_2 + \beta_4 D_1 log_{10}A + \beta_5 D_2 log_{10}A \tag{A.1}$$

Similarly, $Q - A$ the regression equations becomes

$$log_{10}Q = \beta_o + \beta_1 log_{10}A + \beta_2 D_1 + \beta_3 D_2 + \beta_4 D_1 log_{10}A + \beta_5 D_2 log_{10}A \tag{A.2}$$

In doing so, we define the null hypothesis for the similarity of regression coefficient as follows:

Case I: comparing the regression coefficient of the Ganga and Brahmaputra river basin

For exponent:
H_o: $\beta_4 = 0$ (exponent of G and B is similar)
with alternate hypothesis
H_a: $\beta_4 \neq 0$ (exponent of G and B is different)
For intercept:
H_o: $\beta_2 = 0$ (intercept of G and B is similar)
with alternate hypothesis
H_a: $\beta_2 \neq 0$ (intercept of G and B is different)

Case II: comparing the regression coefficient of the Ganga and Indus river basin

For exponent:
H_o: $\beta_5 = 0$ (exponent of G and I is similar)
with alternate hypothesis
H_a: $\beta_5 \neq 0$ (exponent of G and I is different)
For intercept:
H_o: $\beta_3 = 0$ (intercept of G and I is similar)
with alternate hypothesis
H_a: $\beta_3 \neq 0$ (intercept of G and I is different)

Case III: comparing the regression coefficient of the Brahmaputra and Indus river basin

For exponent:

H_o: $\beta_4 = \beta_5$ (exponent of B and I is similar)
with alternate hypothesis
H_a: $\beta_4 \neq \beta_5$ (exponent of B and I is different)
For intercept:
H_o: $\beta_2 = \beta_3$ (intercept of B and I is similar)
with alternate hypothesis
H_a: $\beta_2 \neq \beta_3$ (intercept of B and I is different)

Appendix B. Tables

Table B.6
Summary of the regression coefficients of the rating curve relationship of the discharge and channel width to the catchment area reported in the published literature

Source	Coefficient	Exponent	Catchment area (km^2)	Country
Discharge-catchment area (Q vs. A)				
Syvitski and Milliman (2007)	0.08	0.80	10^2-10^7	World wide
Pavelsky et al. (2014)	0.01	1.00	10^3-10^6	Canada
Mohamoud and Parmar (2006)	0.02-0.04	0.85-0.99	6-10^3	USA
Smoot et al. (2015)	0.04	1.01	17-1700	USA
Rice (1998)	0.16	0.96	10-10^4	Canada
Whiting et al. (1999)	0.06	1.01	1-380	USA
Sodnik and Mikoš (2006)	7-12.5	0.72-0.76	0.56-44.30	Europe
Channel width-Catchment area (W vs. A)				
Frasson et al. (2019)	9.68	0.32	10^3-10^7	World wide
Whitbread et al. (2015)	3.3-5.42	0.35-0.39	<1-500	Scotland
Montgomery and Gran (2001)	0.00-0.05	0.20- 0.60	0.1-10^3	USA
Whipple (2004)	3.3	0.35	0.1-10^3	USA and China
Vianello and D'agostino (2007)	2.66	0.28	0.04-7.08	Italy
Van Der Beek and Bishop (2003)	0.012	0.41	10^2-10^4	Australia
Whiting et al. (1999)	1.23	0.47	1-380	USA

Table B.7
Catchment area and discharge recorded at the gauge station of the different rivers of the Indus, Ganga, and Brahmaputra basins.

River	Longitude	Latitude	Catchment area (km^2)	Average annual discharge (m^{3}s^{-1})	Resolution
Buri Dihing[c]	94.88	27.31	4997	444	Annual
Ravi[b]	75.62	32.37	6257	266	Monthly
Teesta[b]	88.87	26.33	9071	605	Monthly
Jai Bhorili[c]	92.88	26.81	10402	824	Annual
Teesta[b]	89.53	25.7	10628	864	Monthly
Yamuna[a]	77.59	30.32	11396	271	Monthly
Jhelum[b]	74.33	34.21	12543	221	Monthly
Dibang[c]	95.59	27.8	13228	698	Annual
Beas[b]	75.05	31.21	16319	497	Monthly
Chenab[b]	74.74	32.89	22543	797	Monthly
Ganga[c]	78.11	29.64	24005	481	Annual
Subansiri[c]	94.25	27.45	26331	1712	Annual
Lohit[c]	95.61	27.8	26496	1554	Annual
Ganga[a]	78.14	28.76	28923	650	10 daily
Manas[c]	90.92	26.5	29027	1015	Annual
Sutlej[c]	77.12	31.24	51462	1178	Annual
Kosi[b]	87.04	26.53	57974	1560	Monthly
Dihang[c]	95.34	28.08	257008	5644	Annual
Brahmaputra[c]	94.85	27.5	303597	10242	Annual
Brahmaputra[c]	91.74	26.19	415594	14428	Annual
Ganga[c]	81.9	25.41	435562	4126	Annual
Ganga[c]	82.57	25.16	455540	3627	Annual
Ganga[c]	83.01	25.3	457621	4137	Annual
Brahmaputra[c]	90	26.02	469594	16172	Annual
Ganga[c]	83.97	25.57	505707	4436	Annual
Brahmaputra[c]	89.69	25.18	516767	21752	Monthly
Indus[c]	72.24	33.9	534769	3673	Annual
Ganga[c]	85.2	25.62	763954	7626	Annual
Ganga[c]	85.99	25.38	768999	17726	Annual
Ganga[a]	87.24	25.33	805359	8984	10 daily
Ganga[b]	87.94	24.81	926131	11477	Monthly
Ganga[b]	89.02	24.07	941332	12080	Monthly

Sources: *a*: CWC; *b*: GRDD; *c*: Published literature

Table B.8
Catchment area and channel belt width of different rivers of the Indus, Ganga, and Brahmaputra basins.

River name	UTM zone	Longitude	Latitude	Catchment area (km^2)	Channel belt width (m)
Chenab R	43	72.91	31.72	37918	3447
Indus R	42	70.81	31	644625	14438
Jhelum R	43	72.31	32.19	42779	2268
Ravi R	43	75.18	32.11	8497	3053
Ganga R	44	78.27	28.48	29302	2394
Fulahar R	45	87.81	25.71	11333	1812
Gandak R	45	84.33	26.78	39171	7732
Ghaghara R	44	82.26	26.78	84967	3530
Kali nadi/ Sarda R	44	80.49	28.4	16471	3473
Rapti R	44	81.83	27.68	6960	1928
Kosi R	45	86.79	26.44	59331	7892
Kankai R	45	87.74	26.02	2623	1964
Ramganga R	44	79.37	28.32	18216	1648
Yamuna R	43	77.2	29.86	13220	1762
Beki R	46	90.92	26.49	29027	2565
Brahmaputra R	46	92.22	26.46	392016	11161
Torsa R	45	89.34	26.42	4236	1675
Gangadhar R/ Dhubri R	45	89.82	26.08	15518	2451
Dhanshiri R	46	92.26	26.64	1398	1147
Kameng R/ Jia bhoreli R	46	92.88	26.66	10753	3334
————————	46	93.42	26.85	619	952
Dikrong R	46	93.92	27.05	1311	1235
Subansiri R	46	94.09	27.02	32790	3130
Manas R	46	90.66	26.49	1894	2451
Teesta R	45	89.09	26.12	9274	4932
Dharia R/Jaldhaka R	45	89.44	26.04	5448	2156

References

Afshari, S., Fekete, B.M., Dingman, S.L., Devineni, N., Bjerklie, D.M., Khanbilvardi, R.M., 2017. Statistical filtering of river survey and streamflow data for improving at-a-station hydraulic geometry relations. J. Hydrol. 547, 443–454.

Andrews, E.D., 1984. Bed-material entrainment and hydraulic geometry of gravel-bed rivers in Colorado. Geol. Soc. Am. Bull. 95 (3), 371–378.

Ashmore, P., Parker, G., 1983. Confluence scour in coarse braided streams. Water Resour. Res. 19 (2), 392–402.

Bhadra, B.K., Gupta, A., Sharma, J., 2009. Saraswati nadi in Haryana and its linkage with the Vedic Saraswati river-integrated study based on satellite images and ground based information. J. Geol. Soc. India 73 (2), 273–288.

Bhattacharya, J.P., Copeland, P., Lawton, T.F., Holbrook, J., 2016. Estimation of source area, river paleo-discharge, paleoslope, and sediment budgets of linked deep-time depositional systems and implications for hydrocarbon potential. Earth Sci. Rev. 153, 77–110.

Bierman, P.R., Montgomery, D.R, 2014. Key Concepts in Geomorphology. W.H. Freeman and Company, New York, pp. 1–494.

Bookhagen, B., Thiede, R.C., Strecker, M.R., 2005. Late Quaternary intensified monsoon phases control landscape evolution in the Northwest Himalaya. Geology 33 (2), 149–152.

Carling, P., 1988. The concept of dominant discharge applied to two gravel-bed streams in relation to channel stability thresholds. Earth Surf. Process. Landf. 13 (4), 355–367.

CGWB, 2016. Palaeochannels of the North West India: Review and Assessment. Report of the expert committee to review available information on palaeochannels. CWC, New Delhi, pp. 1–115 http://cgwb.gov.in/Ground-Water/Final%20print%20version_Palaeochannel%20Expert%20Committee_15thOct2016.pdf.

Chatterjee, A., Ray, J.S., Shukla, A.D., Pande, K., 2019. On the existence of a perennial river in the Harappan heartland. Sci. Rep. 9 (1), 1–7.

Clift, P.D., Carter, A., Giosan, L., Durcan, J., Duller, G.A., Macklin, M.G., Alizai, A., Tabrez, A.R., Danish, M., VanLaningham, S., et al., 2012. U-pb zircon dating evidence for a Pleistocene Sarasvati river and capture of the Yamuna river. Geology 40 (3), 211–214.

Cohen, J., Cohen, P., West, S.G., Aiken, L.S., 2013. Applied multiple regression/correlation analysis for the behavioral sciences. Lawrence Erlabaum Associates, Landon, pp. 1–691.

Danino, M., 2010. The Lost River: On the Trail of the Sarasvati. Penguin Books India, pp. 1–341.

Dave, A.K., Courty, M.A., Fitzsimmons, K.E., Singhvi, A.K., 2019. Revisiting the contemporaneity of a mighty river and the Harappans: Archaeological, Stratigraphic and Chronometric constraints. Quat. Geochronol. 49, 230–235.

Davidson, S.K., North, C.P., 2009. Geomorphological regional curves for prediction of drainage area and screening modern analogues for rivers in the rock record. J. Sediment. Res. 79 (10), 773–792.

Dixit, Y., Hodell, D.A., Giesche, A., Tandon, S.K., Gázquez, F., Saini, H.S., Skinner, L.C., Mujtaba, S.A., Pawar, V., Singh, R.N., et al., 2018. Intensified summer monsoon and the urbanization of Indus civilization in Northwest India. Sci. Rep. 8 (1), 1–8.

Doll, B.A., Wise-Frederick, D.E., Buckner, C.M., Wilkerson, S.D., Harman, W.A., Smith, R.E., Spooner, J., 2002. Hydraulic geometry relationships for urban streams throughout the piedmont of North Carolina. JAWRA J. Am. Water Res. Assoc. 38 (3), 641–651.

Durcan, J.A., Thomas, D.S., Gupta, S., Pawar, V., Singh, R.N., Petrie, C.A., 2019. Holocene landscape dynamics in the Ghaggar-Hakra palaeochannel region at the Northern edge of the Thar desert, Northwest India. Quat. Int. 501, 317–327.

Dury, G.H., 1976. Discharge prediction, present and former, from channel dimensions. J. Hydrol. 30 (3), 219–245.

Faustini, J.M., Kaufmann, P.R., Herlihy, A.T., 2009. Downstream variation in bankfull width of wadeable streams across the conterminous United States. Geomorphology 108 (3–4), 292–311.

Frasson, R.P.d.M., Pavelsky, T.M., Fonstad, M.A., Durand, M.T., Allen, G.H., Schumann, G., Lion, C., Beighley, R.E., Yang, X., 2019. Global relationships between river width, slope, catchment area, meander wavelength, sinuosity, and discharge. Geophys. Res. Lett. 46 (6), 3252–3262.

Garavaglia, S., Sharma, A., 1998. A smart guide to dummy variables: four applications and a macro. In: Proceedings of the Northeast SAS Users Group Conference., 43 Murry Hill, New Jersey.

Gaurav, K., Métivier, F., Devauchelle, O., Sinha, R., Chauvet, H., Houssais, M., Bouquerel, H., 2015. Morphology of the Kosi megafan channels. Earth Surf. Dyn. 3 (3), 321–331.

Gaurav, K., Tandon, S., Devauchelle, O., Sinha, R., Métivier, F., 2017. A single width-discharge regime relationship for individual threads of braided and meandering rivers from the Himalayan foreland. Geomorphology 295, 126–133.

Geyh, M., Ploethner, D., 1995. An applied palaeohydrological study in Cholistan, Thar desert, Pakistan. Int. Assoc. Hydrol. Sci. Public. 232, 119–127.

Gibling, M.R., 2006. Width and thickness of fluvial channel bodies and valley fills in the geological record: a literature compilation and classification. J. Sediment. Res. 76 (5), 731–770.

Giosan, L., Clift, P.D., Macklin, M.G., Fuller, D.Q., Constantinescu, S., Durcan, J.A., Stevens, T., Duller, G.A., Tabrez, A.R., Gangal, K., et al., 2012. Fluvial landscapes of the Harappan civilization. Proc. Natl. Acad. Sci. 109 (26), E1688–E1694.

Gujarati, D.N., Porter, D.C., Gunasekar, S., 2012. Basic Econometrics. Tata McGraw-Hill Education, New Delhi, pp. 1–873.

Gupta, A., 2020. Introducing Large Rivers. John Wiley & Sons, UK, pp. 1–281.

Gupta, A., Sharma, J., Sreenivasan, G., 2011. Using satellite imagery to reveal the course of an extinct river below the Thar desert in the Indo-Pak region. Int. J. Remote Sens. 32 (18), 5197–5216.

Gupta, A., Sharma, J., Sreenivasan, G., Srivastava, K., 2004. New findings on the course of river Sarasvati. J. Indian Soc. Remote Sens. 32 (1), 1–24.

Hayden, A.T., Lamb, M.P., Fischer, W.W., Ewing, R.C., McElroy, B.J., Williams, R.M., 2019. Formation of sinuous ridges by inversion of river-channel belts in Utah, USA, with implications for mars. Icarus 332, 92–110.

Hesse, P.P., Williams, R., Ralph, T.J., Fryirs, K.A., Larkin, Z.T., Westaway, K.E., Farebrother, W., 2018. Palaeohydrology of lowland rivers in the Murray-Darling basin, Australia. Quat. Sci. Rev. 200, 85–105.

Johnson, P.A., Fecko, B., 2008. Regional channel geometry equations: a statistical comparison for physiographic provinces in the Eastern US. River Res. Appl. 24 (6), 823–834.
Kar, A., 2021. Identification and Mapping of the Saraswati River System: A Review and New Findings in Saraswati. Saraswati: The River Par Excellence (eds by Acharyya S. K, Ghosh.K and Kar A). The Asiatic Society, Kolkata, pp. 29–98.
Kar, A., Ghose, B., 1984. The Drishadvati river system of India: an assessment and new findings. Geogr. J. 221–229.
Khonde, N., Singh, S.K., Maurya, D., Rai, V.K., Chamyal, L., Giosan, L., 2017. Tracing the vedic Saraswati river in the great rann of Kachchh. Sci. Rep. 7 (1), 1–6.
Kolberg, F.J., Howard, A.D., 1995. Active channel geometry and discharge relations of U. S piedmont and midwestern streams: the variable exponent model revisited. Water Resour. Res. 31 (9), 2353–2365.
Kumar, R., Singh, K., Singh, B., Aulakh, S., 2014. Mapping groundwater quality for irrigation in Punjab, North-West India, using Geographical Information System. Environ. Earth Sci. 71 (1), 147–161.
Lecce, S.A., 2013. Stream power, channel change, and channel geometry in the Blue river, Wisconsin. Phys. Geogr. 34 (4–5), 293–314.
Leigh, D.S., Feeney, T.P., 1995. Paleochannels indicating wet climate and lack of response to lower sea level, Southeast Georgia. Geology 23 (8), 687–690.
Leopold, L.B., Maddock, T., 1953. The hydraulic geometry of stream channels and some physiographic implications. US Government Printing Office, Washington, D.C., pp. 1–57. https://doi.org/10.3133/pp252
Maemoku, H., Shitaoka, Y., Nagatomo, T., Yagi, H., 2012. Geomorphological constraints on the Ghaggar river regime during the mature Harappan period. Clim Landsc. Civil. 198, 97–106.
Mehdi, S.M., Pant, N.C., Saini, H.S., Mujtaba, S., Pande, P., 2016. Identification of palaeochannel configuration in the Saraswati river basin in parts of Haryana and Rajasthan, India, through digital remote sensing and GIS. Episodes 39 (1), 29–38.
Miall, A.D., 2006. How do we identify big rivers? and how big is big? Sediment. Geol. 186 (1-2), 39–50.
Miller, Z.F., Pavelsky, T.M., Allen, G.H., 2014. Quantifying river form variations in the Mississippi Basin using remotely sensed imagery. Hydrology and Earth System Sciences 18 (12), 4883–4895.
Mohamoud, Y.M., Parmar, R.S., 2006. Estimating streamflow and associated hydraulic geometry, the Mid-Atlantic region, USA. JAWRA J. Am. Water Res. Assoc. 42 (3), 755–768.
Montgomery, D.R., Gran, K.B., 2001. Downstream variations in the width of bedrock channels. Water Resour. Res. 37 (6), 1841–1846.
Naruse, T., 1985. Aeolian geomorphology of the Punjab plains and the North Indian desert. Ann. Arid Zone 24, 267–280.
O'Callaghan, J.F., Mark, D.M., 1984. The extraction of drainage networks from digital elevation data. Comput. Vis. Graphics Image Process. 28 (3), 323–344.
Orengo, H.A., Petrie, C.A., 2017. Large-scale, multi-temporal remote sensing of palaeo-river networks: a case study from Northwest India and its implications for the Indus Civilisation. Remote Sens. 9 (7), 735.
Pavelsky, T.M., Allen, G.H., Miller, Z.F., 2014. Spatial patterns of river width in the Yukon river basin. In: Remote Sensing of the Terrestrial Water Cycle. (Geophysical Monograph Series 206) American Geophysical Union (AGU) Chapman Conference (eds Lakshmi V., Alsdorf D., Anderson M., Biancamaria S., Cosh M., Entin J., Huffman G., Kustas W., Oevelen PV., Painter T., Parajka J., Rodell M., Rüdiger C.). American Geophysical Union & John Wiley & Sons, Inc, Hoboken, New Jersey, pp. 131–141.
Petrie, C.A., Singh, R.N., Bates, J., Dixit, Y., French, C.A., Hodell, D.A., Jones, P.J., Lancelotti, C., Lynam, F., Neogi, S., et al., 2017. Adaptation to variable environments, resilience to climate change: investigating land, water and settlement in Indus Northwest India. Curr. Anthropol. 58 (1), 1–30.
Potter, P.E., 1978. Significance and origin of big rivers. J. Geol. 86 (1), 13–33.
Radhakrishna, B., Merh, S., 1999. Vedic Sarasvati: evolutionary history of a lost river of Northwestern India. Geological Society of India, pp. 1–329.
Raikes, R., 1968. Kalibangan: death from natural causes. Antiquity 42 (168), 286–291.
Rajawat, A., Sastry, C., Narain, A., 1999. Application of pyramidal processing on high resolution IRS- 1C data for tracing migration of the Sarasvati river in parts of thar desert. In Vedic Saraswati: Evolutionary History of a Lost River in Northwest India (eds Radhakrishna, B. P. and Merh, S. S.), Geological Society of India, Bangalore. Memoirs-Geological Society of India, pp. 259–272.
Rajawat, A., Verma, P., Nayak, S., Rajawat, A., Verma, P., Nayak, S., 2003. Reconstruction of palaeodrainage network in northwest India: retrospect and prospects of remote sensing based studies. Proc. Indian Natl. Sci. Acad. A 69 (2), 217–230.
Rhoads, B.L., 1991. A continuously varying parameter model of downstream hydraulic geometry. Water Resour. Res. 27 (8), 1865–1872.
Rice, S., 1998. Which tributaries disrupt downstream fining along gravel-bed rivers? Geomorphology 22 (1), 39–56.
Roy, D.B., Tandon, S.K., Singh, V., 2021. Drainage evolution in a Holocene landscape that hosted a 'lost river' system in the Punjab-Haryana plains, NW India. Quat. Int. 585, 99–110.
Saini, H., Alok, A., Pant, N., 2020. The lost Saraswati river of Northwestern Indian plains: status and way forward. Episodes J. Int. Geosci. 43 (1), 524–534.
Saini, H., Mujtaba, S., 2012. Depositional history and palaeoclimatic variations at the Northeastern fringe of Thar desert, Haryana plains, India. Quat. Int. 250, 37–48.
Saini, H., Tandon, S., Mujtaba, S., Pant, N., Khorana, R., 2009. Reconstruction of buried channel-floodplain systems of the Northwestern Haryana plains. Curr. Sci. 97 (11.), 1634–1643.
Schäuble, H., Marinoni, O., Hinderer, M., 2008. A GIS-based method to calculate flow accumulation by considering dams and their specific operation time. Comput. Geosci. 34 (6), 635–646.
Scherler, D., Bookhagen, B., Wulf, H., Preusser, F., Strecker, M.R., 2015. Increased Late Pleistocene erosion rates during fluvial aggradation in the Garhwal Himalaya, Northern India. Earth Planet. Sci. Lett. 428, 255–266.
Schumm, S., 1972. Fluvial paleochannels: In recognition of ancient sedimentry environments, edited by J.Keith Rigby, William K. Hamblin. SEPM Special Publication No. 16, Tulsa, Oklahoma, USA, pp. 98–107.
Schumm, S.A., 1968. River adjustment to altered hydrologic regimen, Murrumbidgee river and paleochannels, Australia. Geological Survey Professional Paper 598. US Government Printing Office, Washington, pp. III–65. https://doi.org/10.3133/pp598.
Schumm, S.A., 1985. Patterns of alluvial rivers. Annu. Rev. Earth Planet. Sci. 13 (1), 5–27.
Schumm, S.A., Lichty, R.W., 1965. Time, space, and causality in geomorphology. Am. J. Sci. 263 (2), 110–119.
Singh, A., Jain, V., Danino, M., Chauhan, N., Kaushal, R.K., Guha, S., Prabhakar, V., 2021. Larger floods of Himalayan foothill rivers sustained flows in the Ghaggar-Hakra channel during Harappan age. J. Quat. Sci. 36 (4), 611–627.
Singh, A., Paul, D., Sinha, R., Thomsen, K.J., Gupta, S., 2016. Geochemistry of buried river sediments from Ghaggar plains, NW india: Multi-proxy records of variations in provenance, paleoclimate, and paleovegetation patterns in the Late Quaternary. Palaeogeogr. Palaeoclimatol. Palaeoecol. 449, 85–100.
Singh, A., Sinha, R., 2019. Fluvial response to climate change inferred from sediment cores from the Ghaggar-Hakra paleochannel in NW Indo-Gangetic plains. Palaeogeogr. Palaeoclimatol. Palaeoecol. 532, 1–15.
Singh, A., Thomsen, K.J., Sinha, R., Buylaert, J.P., Carter, A., Mark, D.F., Mason, P.J., Densmore, A.L., Murray, A.S., Jain, M., et al., 2017. Counter-intuitive influence of Himalayan river morphodynamics on Indus civilisation urban settlements. Nat. Commun. 8 (1), 1–14.
Sinha, R., Yadav, G., Gupta, S., Singh, A., Lahiri, S., 2013. Geo-electric resistivity evidence for subsurface palaeochannel systems adjacent to Harappan sites in Northwest India. Quat. Int. 308, 66–75.
Smoot, Z.T, Jayakaran, A.D, Hitchcock, D.R, 2015. Hydraulic geometry curves in the Pee Dee watershed. J. SC Water Res. 2 (1), 63–69.
Sodnik, J., Mikoš, M., 2006. Estimation of magnitudes of debris flows in selected torrential watersheds in Slovenia. Acta geographica Slovenica 46 (1), 93–123.
Sokal, R., Rohlf, F., 1995. Biometry: the principle and practice of statistics in biological research, 103. Freeman W.H, New York, pp. Xiii–915.
Splinter, D.K., Dauwalter, D.C., Marston, R.A., Fisher, W.L., 2010. Ecoregions and stream morphology in Eastern Oklahoma. Geomorphology 122 (1-2), 117–128.
Stein, A., 1942. A survey of ancient sites along the "lost" Sarasvati river. Geogr. J. 99 (4), 173–182.
Syvitski, J.P., Milliman, J.D., 2007. Geology, geography, and humans battle for dominance over the delivery of fluvial sediment to the coastal ocean. J. Geol. 115 (1), 1–19.
Tandon, S.K., Sinha, R., 2007. Geology of large river systems. Large Rivers: Geomorphology and Management (eds by Gupta, A.). John Wiley & Sons, Ltd, West Sussex, England, pp. 7–28.
Valdiya, K., 2016. Prehistoric river Saraswati, Western India. Geological Appraisal and Social Aspects. The Society of Earth Scientists, Springer, Switzerland, pp. V–136.
Van Der Beek, P., Bishop, P., 2003. Cenozoic river profile development in the upper Lachlan catchment (SE Australia) as a test of quantitative fluvial incision models. J. Geophys. Res. Solid Earth 108 (B6), 1–27.
Van Der Beek, P., Champel, B., Mugnier, J.L., 2002. Control of detachment dip on drainage development in regions of active fault-propagation folding. Geology 30 (5), 471–474.
Van Dijk, W., Densmore, A., Singh, A., Gupta, S., Sinha, R., Mason, P., Joshi, S., Nayak, N., Kumar, M., Shekhar, S., et al., 2016. Linking the morphology of fluvial fan systems to aquifer stratigraphy in the Sutlej-Yamuna plain of Northwest India. J. Geophys. Res. Earth Surf. 121 (2), 201–222.
Vianello, A., D'agostino, V., 2007. Bankfull width and morphological units in an Alpine stream of the Dolomites (Northern Italy). Geomorphology 83 (3–4), 266–281.
Whipple, K.X., 2004. Bedrock rivers and the geomorphology of active orogens. Annu. Rev. Earth Planet. Sci. 32, 151–185.
Whitbread, K., Jansen, J., Bishop, P., Attal, M., 2015. Substrate, sediment, and slope controls on bedrock channel geometry in postglacial streams. J. Geophys. Res. Earth Surf. 120 (5), 779–798.
Whiting, P.J., Stamm, J.F., Moog, D.B., Orndorff, R.L., 1999. Sediment-transporting flows in headwater streams. Geol. Soc. Am. Bull. 111 (3), 450–466.
Wilkerson, G.V., Parker, G., 2011. Physical basis for quasi-universal relationships describing bankfull hydraulic geometry of sand-bed rivers. J. Hydraul. Eng. 137 (7), 739–753.
Wolman, M.G., Miller, J.P., 1960. Magnitude and frequency of forces in geomorphic processes. J. Geol. 68 (1), 54–74.
Xu, J., Snedden, J.W., Galloway, W.E., Milliken, K.T., Blum, M.D., 2017. Channel-belt scaling relationship and application to Early Miocene source-to-sink systems in the gulf of Mexico basin. Geosphere 13 (1), 179–200.
Yashpal, B., 1980. Remote sensing of the lost Saraswati river. Proc. Indian Acad. Sci. 89, 317–337.